Title
Design and Performance of the ALS diagnostic Beamline

Journal
Review of Scientific Instruments, 67(9)

Authors
Renner, T.R.
Padmore, H.
Keller, R.

Publication Date
1995-09-21

LBL-37638
UC-410

Lawrence Berkeley Laboratory
UNIVERSITY OF CALIFORNIA

Accelerator & Fusion Research Division

To be presented at the National Conference on Synchrotron Radiation Instrumentation, Argonne, IL, October 17–20, 1995, and to be published in the Proceedings

Design and Performance of the ALS Diagnostic Beamline

T. Renner, H.A. Padmore, and R. Keller

September 1995

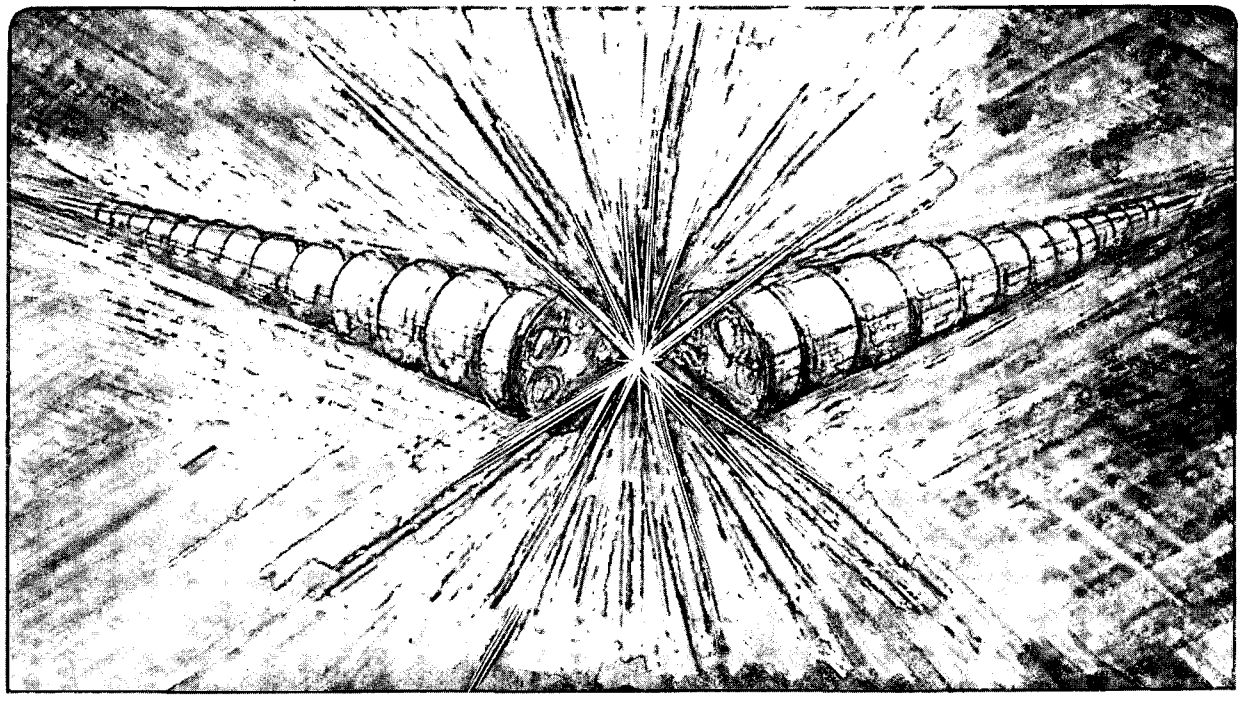

Prepared for the U.S. Department of Energy under Contract Number DE-AC03-76SF00098

DISCLAIMER

LBL-37638
LSBL-274
UC-410

Design and Performance of the ALS Diagnostic Beamline

T. Renner, H.A. Padmore, and R. Keller

Advanced Light Source
Accelerator and Fusion Research Division
Lawrence Berkeley National Laboratory
University of California
Berkeley, California 94720

September 1995

This work was supported by the Director, Office of Energy Research, Office of Basic Energy Sciences, Materials Sciences Division, of the U.S. Department of Energy under Contract No. DE-AC03-76SF00098.

Design and Performance of the ALS Diagnositic Beamline

T.R. Renner, H.A. Padmore, R. Keller

Lawrence Berkeley National Laboratory, University of California, Berkeley, CA 94720

September 22, 1995

The design and operation of an imaging beam line at the Advanced Light Source used for providing diagnostic information on the electron beam for the accelerator and experimental groups is described. This system is based on a Kirkpatrick-Baez mirror pair and utilizes a carbon filter to give a bandpass in the soft x-ray region. The focused x-rays are viewed on a single crystal scintillator through an optical microscope and the image recorded on a CCD camera. This system, together with other instruments to evaluate beam size, stability, and other time-dependent information is described, data is presented, and the operation of the overall beam line is evaluated.

1. INTRODUCTION

Synchrotron light sources have evolved from accelerators which produced this radiation as a by-product to dedicated, third generation storage rings such as the Advanced Light Source (ALS). Optimization of beam line designs to take advantage of these new sources requires information on electron beam parameters and their stability. A real-time, image of the electron beam is useful to accelerator physicists in helping their understanding of beam dynamics, monitoring of accelerator operation, and providing a means of diagnosing problems as they arise. A diagnostic beam line for these purposes has been built at the ALS to image the electron beam by focusing bend magnet radiation.[1] Measurement of beam parameters, electron-bunch time structure and beam dynamics can now be routinely made. The image of the electron beam can be continuously monitored via standard video equipment and the size and location of the beam redundantly measured via a second detection system utilizing a slit scanned in front of a photocathode. Longitudinal electron bunch lengths can be measured with a port providing visible light to an optical platform on which a fast photodiode or a streak camera can be mounted. An additional set of diagnostic tools built into the beam line allows determination of the acceptance of the beam line and the locations of the vertical and horizontal focal planes of the system. The system also provides a discrete method of attenuating the photon flux for equalizing the signal on the video system over the wide range of expected accelerator operating conditions.

The components of the beam line include a Kirkpatrick/Baez[2] pair of focusing mirrors inside the storage ring shield wall and an endstation located outside the shield wall. Figure 1 shows a schematic of the beam line layout. The mirror pair is located in a vacuum vessel with an aperture on its upstream end which defines the system's angular acceptance. The endstation has two parts. The upstream end provides a means of measuring the "filling" of the mirror by the synchrotron light, a method of attenuating the light reaching the downstream end of the endstation, a filtering mechanism for elimination of light less than around 250 eV, and a periscope to deflect visible light upward through a visible light port and then parallel to the beam line. The downstream portion of

the endstation contains devices for measuring and viewing the image. In particular a scintillating crystal converts the broad spectrum x-rays into a visible image that is viewed through a visible light port by a microscope connected to a video camera. Beam size and position can also be measured at this location by scanning slits in front of a photocathode.

2.0 BEAMLINE DESIGN

2.1 Beamline Optics

The horizontal mirror of the Kirkpatrick/Baez mirror pair is located equidistant between the source and image for one-to-one imaging, thus eliminating coma. A summary of the optics is given in Table I. The ALS metrology lab has performed the measurements of slope errors, surface roughness, and curvature included in this table.

The calculated power striking the first mirror is 6.4 Watts at 1.5 GeV, 400 mA operation. Of this, 4.0 watts are absorbed by the mirror and must be removed. Thermal calculations showed that radiative cooling alone would have been barely sufficient for staying within reasonable slope error tolerances at 1.5 GeV, and clearly inadequate at 1.9 GeV.[3] Therefore cooling channels were built into the Glidcop mirror base to allow cooling of the mirror with water.[4] The copper substrate was nickel plated and polished.

The first mirror is vertically downward deflecting and allows beam line operation during injection. The angle and size of penetration through the shield wall eliminates the possibility of user exposure to Bremsstrahlung created from electron beam losses in the accelerator. The ability to image during injection has already been of great improtance in understanding and optimizing the injection process.

2.2. Optical Performance Analysis

The performance of the beam line is determined by the performance of the optics, the effects of alignment errors, and source motion. An analysis was done on each of these effects to ascertain the operational envelope of the system. A change of 1 % in the mirror radius changes the longitudinal location of the image plane by 2%, or 120 mm corresponding to roughly a doubling of

the beam size in the horizontal direction. Figure 2 shows the size of the caustic of the rays calculated with SHADOW [5] as a function of their distance from the nominal focal position.

Changes in vertical mirror angle of 0.25 mrad affect the image in a similar fashion. In the vertical plane a 1 mm steering error would cause the beam size to appear increased by 100 μm. Careful determination of the actual focal plane is therefore necessary prior to regular operation of the beam line. A second concern in designing the optics for this beam line were third order aberrations which would increase the vertical image size, if the magnification in this plane were different from unity. Calculations gave less than a 20 μm contribution to the image size in the vertical plane from the most important aberration, coma for the maximum anticipated source motion.

2.3 Mirror Design

To achieve an easy and accurate method of alignment, free from any significant low frequency vibration, the optics were mounted to a platform which is supported by a six strut support system allowing essentially independent adjustment of the mirror in 6 degrees of freedom. A vacuum tank encases the optics and their base and rests on the platform. Measurement of the mirror positions in the tank with respect to the fiducials mounted on the top of it were made before installation of the entire system in the accelerator tunnel. Alignment of the tank in the tunnel with respect to the building monuments was done using these fiducials. Externally actuated pitch adjustment of the mirrors inside the tank was provided to assure astigmatic operation. Submicroradian adjustment of the vertical mirror angle is possible, bringing its focal plane to the same point as that of the horizontal mirror.

3.0 DIAGNOSTIC EQUIPMENT

3.1 Scanning Slits

The beam at 4 meters from the center of the horizontally deflecting mirror is out of focus and can be used for measurement of the filling of the mirors. Horizontal and vertical translating slits located in front of an Al_2O_3 photocathode at this location are used to measure the beam size. The

slits are 200 μm wide and 10 mm long and aligned orthogonally to each other to within 5 μm. The knife edges of the slits and the photocathode are electrical connected to the outside of the vacuum chamber via SHV connectors. A second set of slits is mounted next to the first set for use with a photocathode at the end of the beam line. The slit scanning and photocurrent measurement are computer controlled to provide measurements of the photocurrent as a function of the slit position.

3.2 Time Dependent Measurements

Visible light is reflected into a vertical port by an aluminum coated silicon wafer, as shown in Figure 1, that can be inserted into the beam via a translation stage. The light is transmitted through an ordinary glass window to a second mirror which deflects it parallel to an optical table. Insertion of the mirror into the beam path precludes imaging the source downstream.

3.3 Filters

To achieve the desired spatial resolution, diffraction effects must be small compared to the smallest beam size expected. Since the desired resolution is on the order of 10 μm or less and the limiting aperture of the system is 1.0 mrad, wavelengths less than 10 nm are required. A simple carbon filter is used to remove light with longer than 10 nm wavelengths. Filters from 20 μm to 0.1 μm in steps of roughly a factor of two allow attenuation of the photon flux by approximately a factor of 10 for each step. The foils themselves are either pyrolytic graphite [6] for the thicker foils (> 5 μm) or evaporated carbon. The foil thickness is chosen to improve the signal to noise ratio and prevent saturation of the charge couple device (CCD). The flux attenuation after two reflections from the nickel coated mirrors and a 5 μm thick carbon foil was calculated using XCAL[7] and is shown in Figure 3.

3.4 Downstream Endstation Section

A second set of slits, similar to the ones discussed above, is available to measure the beam size at or near the focal plane position. A 5 μm carbon foil to filter out diffracted light is mounted upstream of a single slit and a photocathode is mounted downstream of it to convert the transmitted photons into an electrical current. These downstream slits are ~20 μm wide which amounts to approximately 5 to 20 % of the beam width depending on the plane being measured.

The vacuum cross in which the second slit devices are located is mounted to a translation table capable of moving 50 cm collinearly with the beam axis and is connected to the beam line via a long bellows. Measuring the beam size as a function of the position along the beam line allows determination of the location of the focal plane in the two orthogonal directions. Astigmatic imaging is achieved by adjusting the vertical focal plane to coincide with the horizontal focal plane, as discussed in section 2.3.

3.5 Image Viewing System

For viewing the two-dimensional beam profile, a scintillating screen is located in the beam's path in front of a glass window at the end of the beam line. The scintillator is a 25 μm by 25 μm single crystal of bismuth germinate (BGO). The maximum power at 1.5 GeV and 400 mA of electron beam current that can be deposited on the BGO is about 2.6 watts corresponding to a power density of about 165 W/mm^2. The maximum power that the glass window can dissipate without melting is in the order of 30 W/mm^2.[8] Heat loads of this magnitude will lead to rapid temperature changes in the glass, and could cause its fracture. With the appropriate filter in place the power is sufficiently reduced for safe absorption by the BGO crystal or the glass window.

To provide remote viewing of the scintillator image a microscope with a magnification of four is connected to a CCD camera and mounted outside the vacuum on a xyz translator stage for easy adjustment of the microscope focus and the viewing area. The photon flux reaching the CCD camera was calculated by integrating the theoretical flux distribution over the vertical opening angle and taking into account mirror reflectivities, carbon foil flux attenuation, microscope acceptance and the characteristics of the CCD. A 10 μm foil for attenuating the photon flux prevents saturation of the CCD at full electron beam current (400 mA) at 1.5 GeV and a 1 μm thick foil provides a good signal-to-noise ratio at the minimum electron beam current used for diagnostic purposes, (0.1 mA).

4. BEAM LINE CHARACTERIZATION

4.1 Fundamental Parameters

During commissioning, a series of measurements was made to determine the beam line performance. During this time the longitudinal damping system of the storage ring was not operating. First the photocurrent from a downstream photocathode, illuminated by the photon flux collimated with an upstream slit and attenuated by a 5 μm carbon foil, was measured at 1.5 GeV and 400 mA of electron beam current. The calculated photocurrent under such conditions was expected to be 448 nA which is less than the 557 nA actually measured. Uncertainties in the actual slit width, the carbon filter thickness, the mirror reflectivity, and the beam line acceptance could be responsible for this unlikely discrepancy, with the slit width and the carbon foil thickness being the most likely. Next the actual vertical and horizontal beam profiles were measured upstream of the focal plane to determine the degree of mirror filling. The measured size of the beam agreed with expectations confirming the alignment of the system to the source.

Measurement of the vertical focal plane position was made by measuring the vertical beam size with the downstream slits as a function of slit position along the beam line axis. A fit to each distribution was made with a Gaussian plus a linear function to account for the slow decrease seen in the data. A plot of these vertical distribution widths as a function of slit location showed the vertical focal plane located within 100 μm of the horizontal focal plane. Measurements in the horizontal plane were made in similar fashion to those in the vertical plane. Figure 4 shows the profile of the beam at the expected focal plane location and the fit to the data as discussed above. A plot of the beam profile as a function of the longitudinal location shows the depth of field is on the order of 40 cm for a 10% change in beam size.

4.1 Mirror Angle Adjustment

The adjustment to make the system astigmatic was made by varying the vertical mirror angle and measuring the vertical beam size at the location of the horizontal focus. Figure 5 shows the Gaussian widths of the vertical beam extracted from the fits to the data as a function of the per cent change in the grazing angle, which was nominally 1.5 degrees. The angle of the mirror necessary to give an astigmatic image was in fact the nominal angle at installation.

5. BEAM LINE USE

After the initial characterization and optimization of the beam line performance, measurements of the vertical and horizontal beam sizes were made in both single and multibunch operation modes of the accelerator. The transverse beam size (σ) in single bunch mode was 53 μm horizontal by 25 μm vertical as obtained from the CCD camera output. With the beta functions and dispersion functions at this location in the storage ring given below in Table II [9], the horizontal and vertical emittances of the beam have been determined to be 5×10^{-9} m-rad and 3×10^{-11} m-rad, respectively. Using these emittances along with the measured horizontal and vertical multibunch beam sizes of 215 μm by 25 μm respectively an energy spread, $\Delta p/p$, of 0.7% was deduced. This is larger than the single bunch energy spread given in Table 2 and is attributed to a coupled bunch instability in the storage ring in multibunch mode. In addition, the beam image showed a slightly tilted shape indicative of finite vertical dispersion. This vertical dispersion has since been eliminated by changing sextupole and corrector magnet settings.

Changes in the vertical beam size have also been observed while undulator gaps were varied with the existing, feedforward orbit compensation system switched off. Commissioning of the longitudinal feedback system, developed to reduce the energy spread of the machine, has also made extensive use of the diagnostic beam line. The onset of transverse instabilities could be identified by fluctuating changes in vertical beam size. Longitudinal instabilities have been discerned by the growing horizontal beam size arising from an increased energy spread of the electron beam. Figure 6 shows the transverse beam size with the longitudinal and vertical feedback systems working.

Another use of the diagnostic beam line has been to study the vertical size of the beam as a function of the current in a single bunch. The length of a single bunch in time was also measured with a streak camera as a function of the current in the bunch and compared with theoretical predictions.[10] Measurements of bunch length in multibunch mode have been made with and without the longitudinal feedback system operating. A measurement of the temporal length of an electron bunch has also been made on the visible light port using a fast photodiode. Streak camera

measurements determined that the filling of nearby buckets in single bunch operation was less than one part in 3000. Currently electron beam motion is being studied to find correlations with changes in various accelerator parameters.

6. SUMMARY

The performance of the diagnostic beam line has exceeded all design expectations. This beam line is now an integral part of the instrumentation being used in routine operations as well as for dedicated accelerator experiments. The size of the beam can be monitored with electron beam currents from 0.1 mA to 400 mA and for 1.0 to 1.9 GeV with a simple change of carbon foils. The beam centroid position and beam sizes can be continuously tracked during routine operation. Beam size measurements have assisted in the commissioning of the longitudinal and transverse feed back systems on the ALS. Measurements of the electron bunch length using visible light from the diagnostic beam line have also added to the understanding of the performance of the storage ring.

ACKNOWLEDGMENTS

The authors wish to express their gratitude to the ALS technical staff and to the following individuals who helped build this beam line: Pat McKean, Keith Franck, John Thomson, Dan Colomb, Wayne Ogelsby, Ed Wong, Ed Melczer, Cory Lee, Don Gourdain, Charlie Knopff, Richard DeMarco, Alex Gavidia, Steve Irick, TiHowe Guai, Kan Zhu, Arash Saffarina, and Dexter Massoletti. We also wish to thank John Corlett and John Byrd for providing an image of the beam taken during their work on the feedback systems.

This work was supported by the Director, Office of Energy Research, Office of Basic Energy Sciences, Materials Sciences Division, of the U.S. Department of Energy, under Contract No. DE-AC03-76SF00098.

FIGURE CAPTIONS

Fig 1. Schematic of the beam line functions.

Fig. 2 Depth of field calculation for the diagnostic beam line. The lines show the nominal size.

Fig. 3 Photon flux transmission after two reflections and passage through a 5 mm carbon foil.

Fig. 4 Horizontal profile of the beam at the expected focal plane location. The symbols are the data and the heavy solid line is the fit to the data. The straight line indicates the background.

Fig. 5 Vertical beam widths extracted from Gaussian fits to the measured profiles as a function of the change in grazing angle. The data are fitted by a parabola (solid curve).

Fig. 6 ALS diagnostic beam line image showing transverse beam size with vertical, horizontal, and longitudinal feedback systems working at 1.5 GeV beam energy with 400 mA of current. The vertical fiducials are 1.5 mm apart.

REFERENCES

1. R. C. C. Perera, M. E. Melczer, A. Warwick, A. Jackson, B. M. Kincaid, Rev. Sci. Instrum. **63**, 1 (1992).

2. P. Kirkpatrick, A. V. Baez, J. Opt. Soc. Am. **38**, 766 (1948).

3. T. Warwick, S. Sharma, Nucl. Instr. and Meth. in Phys. Res. **A319** 185 (1992).

4. R. DiGennaro, R. Swain, Nucl. Instr. and Meth. in Phys. Res. **A291** 313 (1990).

5. C.Welnak, G. J. Chen, F. Cerrina, Nucl. Instr. and Meth. in Phys. Res. **A347** 344 (1994) .

6. Specialty Minerals Inc., 640 North 13th St. Easton, PA 18042.

7. XCAL is a registered trademark of the Oxford Research Group, 5737 Clinton Ave., Richmond, CA 94805.

8. M. Yoshimatsu and S. Kozaki, *Topics in Applied Physics , X-Ray Optics Applications to Solids* (Springer-Verlag, Heidelberg,1977).

9. ALS Conceptual Design Internal Report Pub-643 Rev. 2, Lawrence Berkeley National Laboratory (1989).

10. J. M. Byrd, J. N. Corlett, T. Renner, Proceeding of the 1995 Particle Accelerator Conference, Dallas, TX.

TABLES

Table I. Optics Parameters

Mirror	Horizontal	Vertical
Grazing Angle	1.5°	2.0°
Slope error RMS	1.53 μrad	1.9 μrad
Surface Roughness RMS	7.7 Å	5.7 Å
Distance to Source	6.1 m	5.7 m
Distance to Image	6.1 m	6.5 m
Radius of Curvature	170.9 m	229.6 m
Size LxWxH	300 x 50 x 50 mm^3	420 x 50 x 50 mm^3
Clear Aperture LxW	400 x 40 mm^2	280 x 40 mm^2

Table II. Theoretical Electron Beam Parameters for the ALS

β_x	β_y	D_x	D_y	$\Delta p/p$
0.404 m	19.90 m	0.030 m	0.0 m	0.08 %

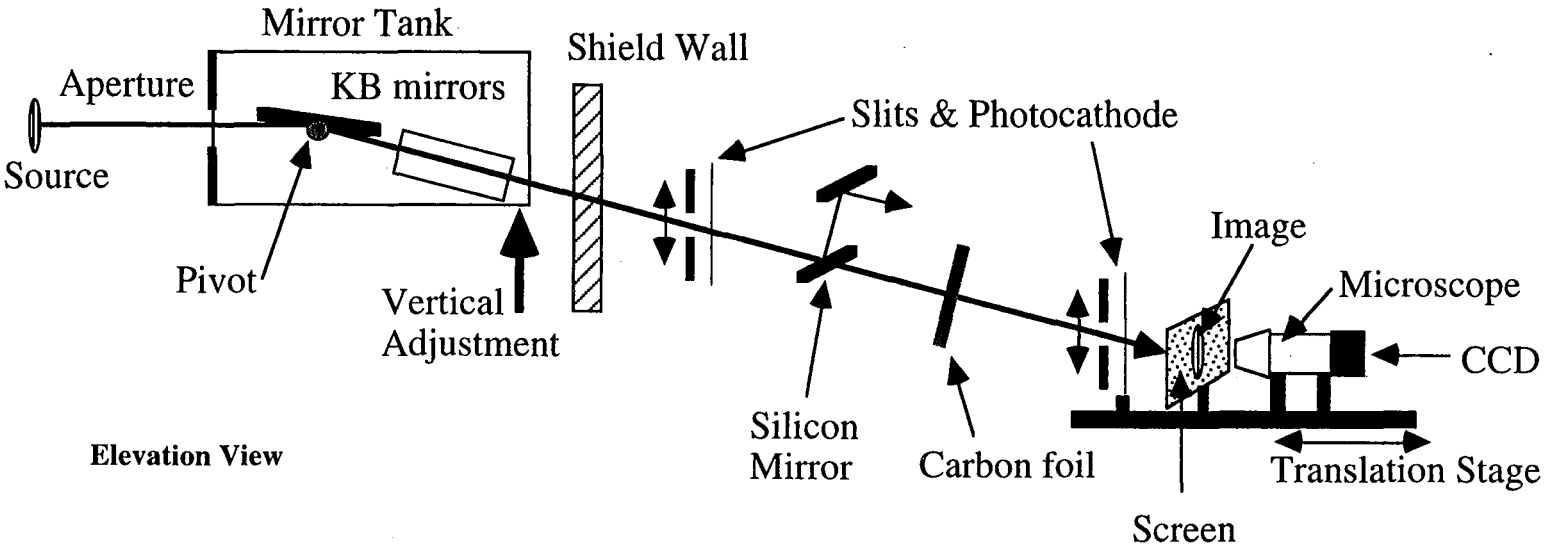

Elevation View

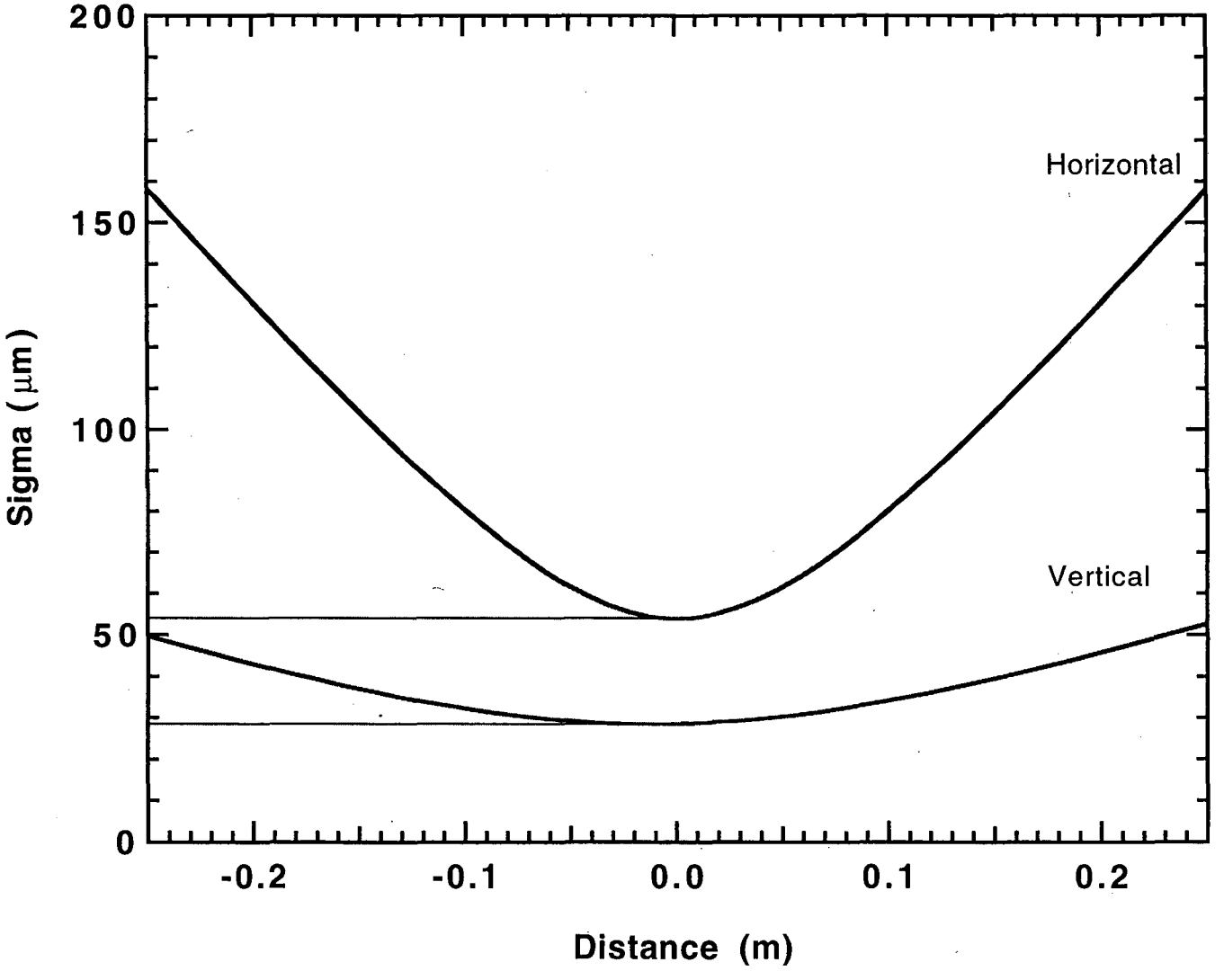
200
150
100
50
0
Sigma (μm)
Horizontal
Vertical
-0.2
-0.1
0.0
0.1
0.2
Distance (m)

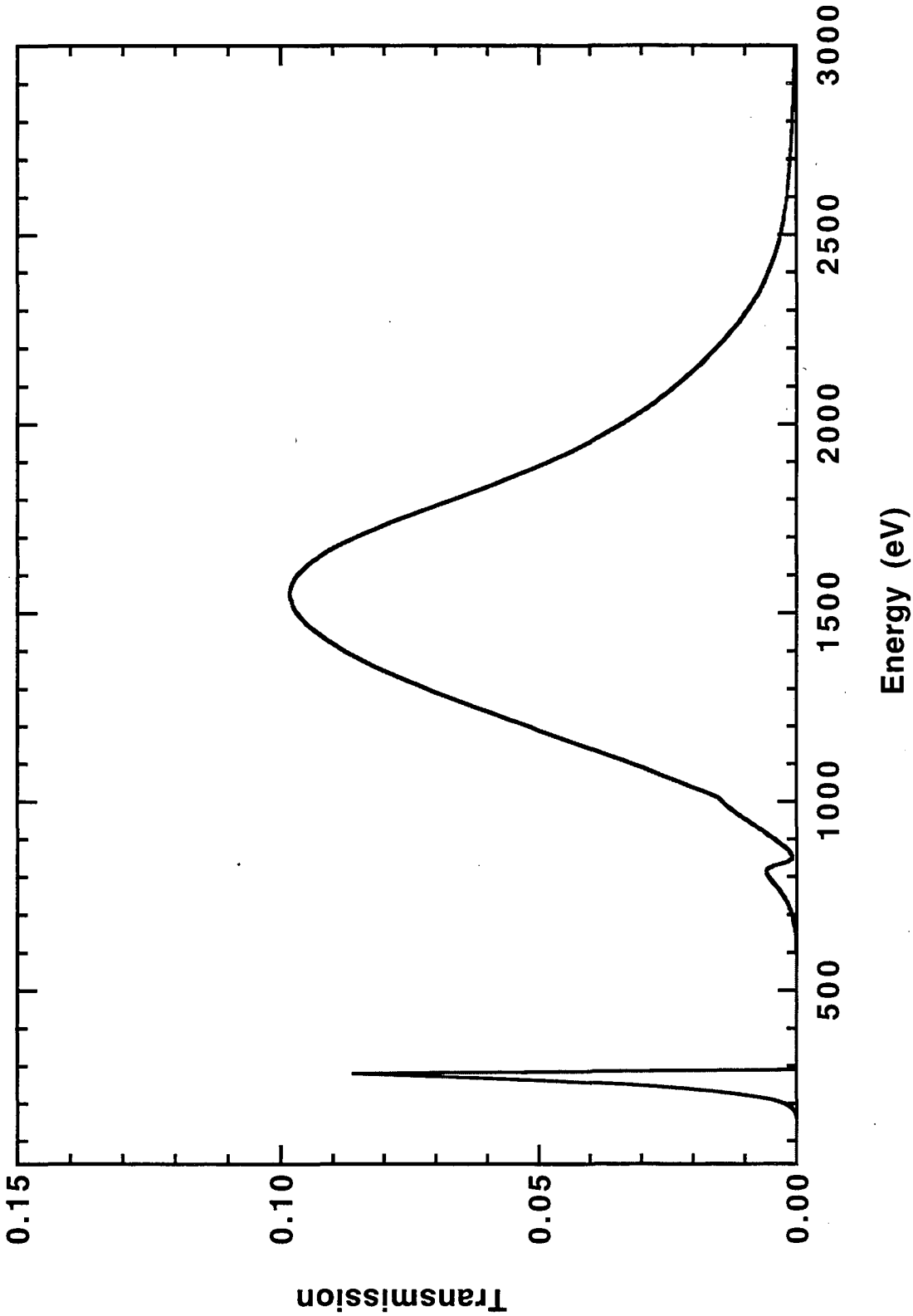
Transmission
0.15
0.10
0.05
0.00
500
1000
1500
2000
2500
3000
Energy (eV)

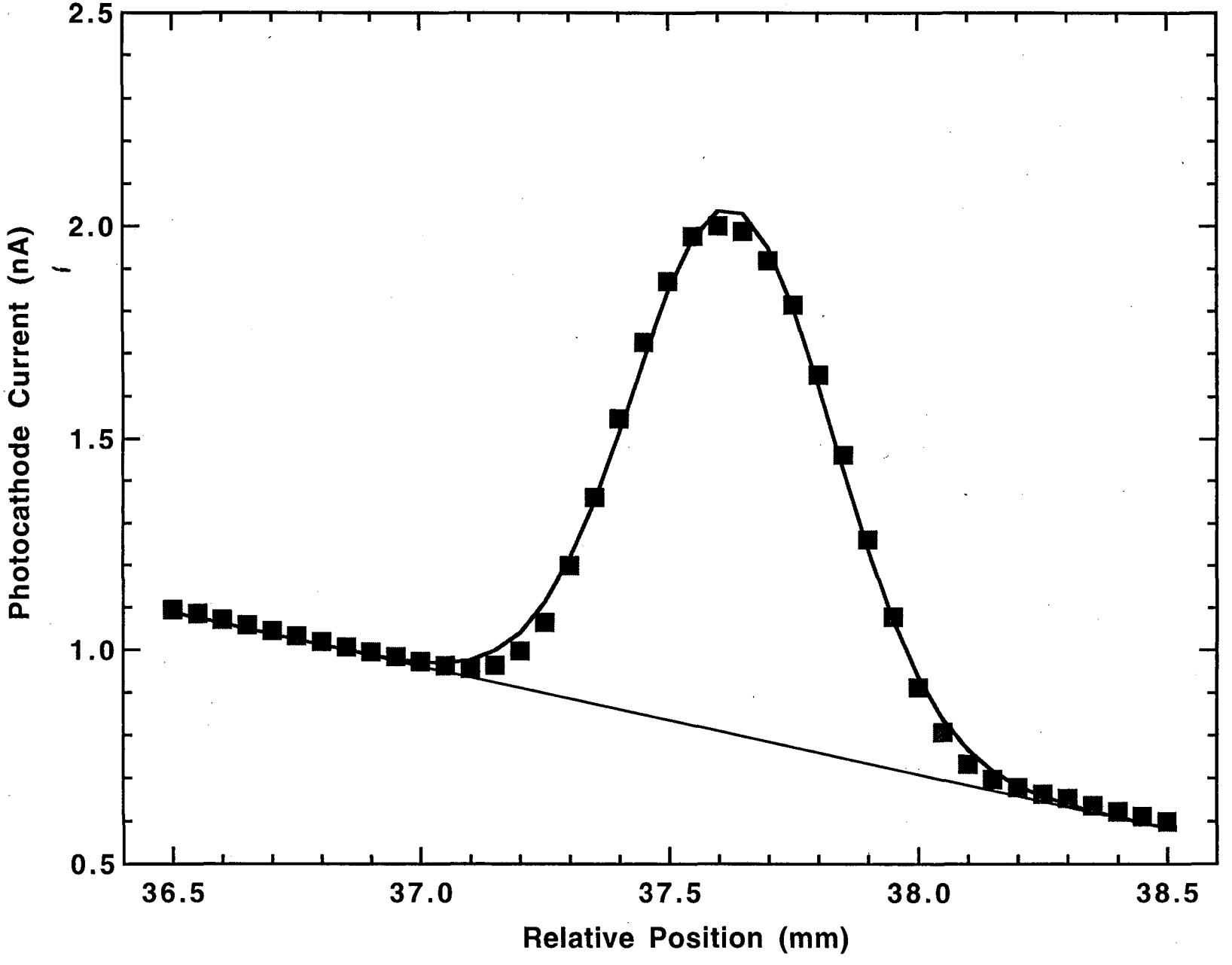
2.5
2.0
1.5
1.0
0.5
Photocathode Current (nA)
36.5
37.0
37.5
38.0
38.5
Relative Position (mm)

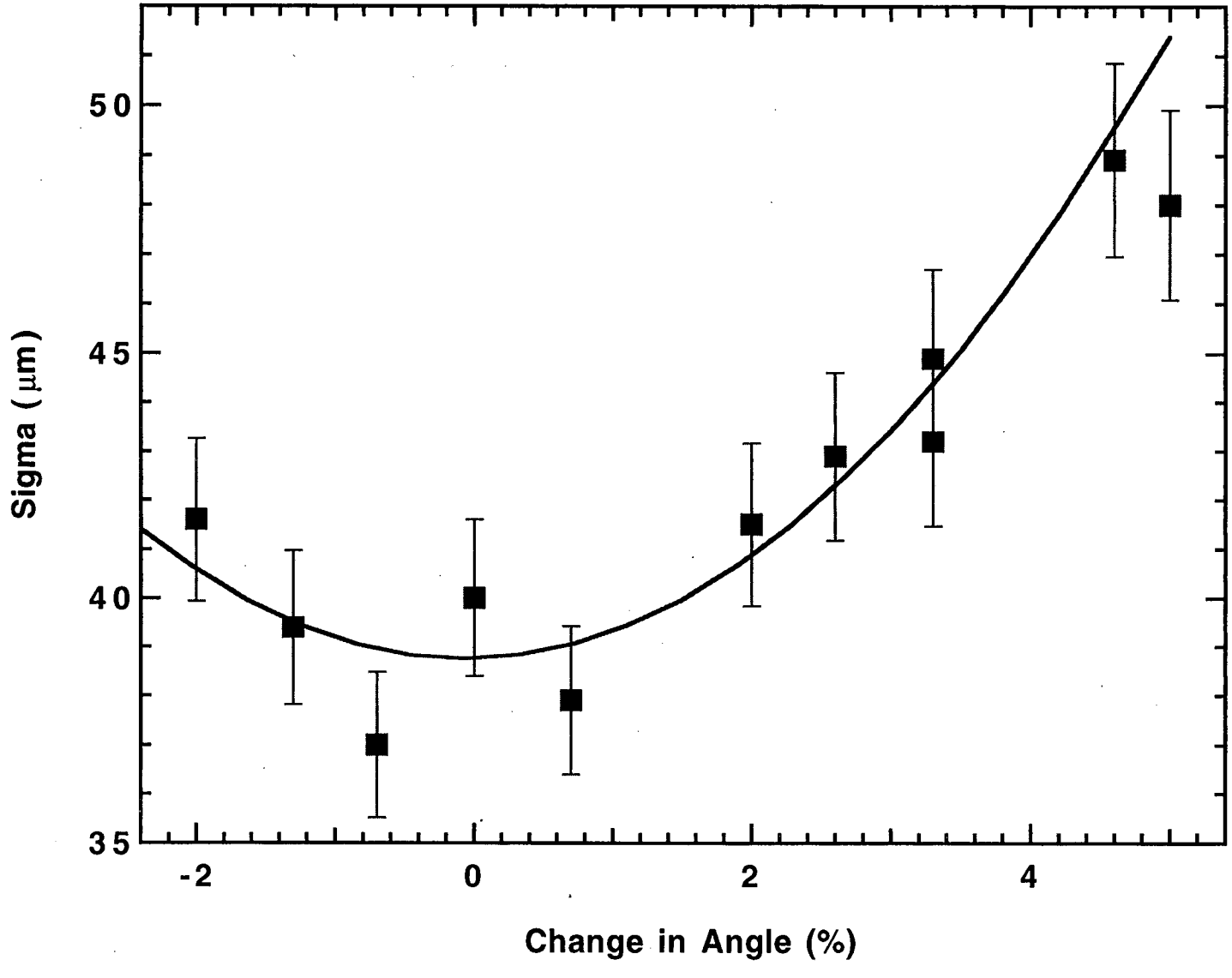
50
45
40
35
Sigma (μm)
-2
0
2
4
Change in Angle (%)

LAWRENCE BERKELEY NATIONAL LABORATORY
UNIVERSITY OF CALIFORNIA
TECHNICAL & ELECTRONIC INFORMATION DEPARTMENT
BERKELEY, CALIFORNIA 94720